

SciEn Conference Series: Engineering Vol. 3, 2025, pp 582-587

https://doi.org/10.38032/scse.2025.3.149

Numerical Analysis of Bicycle Frame Using FEM

Md. Shaiful Islam*, Md. Shahidul Islam

Department of Mechanical Engineering, Khulna University of Engineering & Technology, Khulna-9203, Bangladesh

ABSTRACT

Bicycles are popular mode of transportation around the world. The frame is an important part of a bicycle, which comprises various parts including the top tube, bottom tube, seat tube, chain stay, seat stay, and head tube. The commonly used bicycle frame is diamond shaped. Extensive research has been conducted on the overall frame of different shaped sports bicycle using different materials. However, there are opportunities to conduct detailed research on individual frame tubes under a variety of load conditions. Such investigations could provide deeper insights into the stress distribution, deformation characteristics, and failure mechanisms of each tube. Using finite element analysis, this paper investigates the comparative behavior of each tube of a diamond-shaped bicycle frame using three different materials: Steel, Aluminum 6061-T6 and Titanium alloy. Three load conditions - static start up, horizontal load and vertical load are considered for the analysis. This analysis examines the stresses, that occur within the bicycle frame tubes and indicate that, steel tubes show superior performance in handling both stress and deformation comparing to aluminum and titanium tubes. The analysis reveals that, steel tubes exhibit approximately 65% less deformation compared to aluminum tubes and 51% less deformation compared to titanium tubes. Among the frame components, the seat stay, seat tube, and top tube experience the highest levels of deformation for all load cases. Also, the results show that, strain energy is highest in steel tubes, while aluminum tubes exhibit the lowest strain energy.

Keywords: Finite Element Analysis, Bicycle Frame Analysis, Ansys Structural, Bicycle Tubes



Copyright @ All authors

This work is licensed under a Creative Commons Attribution 4.0 International License.

1. Introduction

Bicycles are used for transportation, recreation and even for sports. There are twice as many bicycles as cars around the world, and their sales is three times more than cars. The first bicycle was built by Baron Karl in Germany in 1817. Since the first chain-driven model was constructed in 1885, various types of bicycles have been made, but the basic look and arrangement in the form of a conventional upright or safety bicycle has altered little. At present, the most popular bicycle frame is diamond shaped. Rajeev Gupta and Seshagiri Rao [1] conducted a comparative analysis on bicycle frames made of Aluminum 6061-T and Aluminum 7005-T. The behavior of a standard bicycle frame made of Magnesium alloy (AZ91D) are compared with the analysis of a bicycle frame made of Aluminum 6061-T6 by Sajimsha et al. [2]. The uses of finite element method to simulate the behavior of typical steel bicycle frames under a variety of stress scenarios is described by Derek Covill et al. [3]. They concluded that, for getting better understanding about tube profiles, selection and load distribution between tubes further research is needed. Designing, testing and stress analysis of a double cradle frame chassis is performed by Shubham Kurhade et al. [4]. Akhyar et al. [5] analyzed the stress and displacement of "T" and "I" profile bicycle frame using both finite element analysis and simple truss structure mechanism. Mahanthesh et al. [6] done both the static and the modal analysis for understanding the frame's dynamic behavior. Arun and Sreejith [7] investigated the structural performance of a bicycle frame. They proposed an optimum ply design for various loading scenarios based on the maximum stress criteria. Rahul and Kishor [8] performed a vibrational analysis of bicycle chassis. They used finite element approach to estimate the dynamic features of bicycle

chassis such as natural frequency and mode shape. They used the bicycle frame made of mild steel and aluminum. Devaiah et al. [9] performed stress analysis on a frame using Ansys software and compared the results with theoretical predictions. The findings showed that, all of the stresses observed in the analysis are significantly below the yield stress of the material that used for the analysis. Krishan and Vedansh [10] analyzed the stress, strain and deformation of a bicycle frame made of aluminum alloy (6061 Al series of 6000) under different conditions. Two simulation methodologies (linear static analysis and fatigue using harmonic analysis) are compared with the experimental results by Kailas et al. [11]. A parametric finite element analysis on road-driven regular bicycle frames with beam element and load profiles were performed by Derek et al. [12]. A finite element analysis was done by Sarath et al. [13] to compare the performance of a bicycle frame made from Steel, Aluminum 6061 T6, Titanium grade 9, and Carbon fiber under various load conditions.

At present, no detailed analysis exists that examine the behavior of individual frame tubes in a bicycle frame under varying load conditions. This paper focuses on investigating the comparative behavior of each tube in a diamond-shaped bicycle frame for different materials under different load conditions. This approach aims to provide deeper perception into the relationship between bicycle frame material selection, tube behavior, and frame durability.

2. Computational Modeling

2.1 Governing Equation

The strain of the tubes for x, y, and z directions can be determined by the following equations.

$$\varepsilon_{x} = \frac{\sigma_{x}}{E} - \frac{v\sigma_{y}}{E} - \frac{v\sigma_{z}}{E} \tag{1}$$

$$\varepsilon_{y} = -v \frac{\sigma_{x}}{E} + \frac{\sigma_{y}}{E} - \frac{v \sigma_{z}}{E} \tag{2}$$

$$\varepsilon_z = -v\frac{\sigma_x}{E} - v\frac{\sigma_y}{E} + \frac{\sigma_z}{E} \tag{3}$$

The properties are unchanging in all directions for an isotropic material. The stress for those types of three-dimensional material is determined by Daryl L. Logan [14] as follows.

$$\begin{pmatrix} \sigma_{x} \\ \sigma_{y} \\ \sigma_{z} \\ \tau_{xy} \\ \tau_{yz} \\ \tau_{zx} \end{pmatrix} = \frac{(1+v)}{(1+v)} \begin{bmatrix} 1-v & v & v & 0 & 0 & 0 & 0 \\ v & 1-v & v & 0 & 0 & 0 & 0 \\ v & v & 1-v & 0 & 0 & 0 & 0 \\ 0 & 0 & 0 & \frac{1-2v}{2} & 0 & 0 & 0 \\ 0 & 0 & 0 & 0 & \frac{1-2v}{2} & 0 & 0 \\ 0 & 0 & 0 & 0 & 0 & \frac{1-2v}{2} & 0 \\ 0 & 0 & 0 & 0 & 0 & \frac{1-2v}{2} & 0 \\ \end{pmatrix} \begin{pmatrix} \varepsilon_{x} \\ \varepsilon_{y} \\ \varepsilon_{x} \\ \gamma_{0} \\ \gamma_{x} \end{pmatrix}$$
 (4)

2.2 Model of Analysis

The CAD model of the bicycle frame is developed using SolidWorks 2018. Table 1 represents the dimensions of the bicycle frame. These dimensions are taken from the website of Precision WATERFORD cycles, USA [15]. Fig. 1 and 2 show the sketch model and 3D model of the bicycle frame.

Table 1 Dimensions of the bicycle frame.

Tube	Parameters	Values (mm)
Top Tube	Length	570
	Outer Diameter	30
	Thickness	2
Bottom Tube	Length	575
	Outer Diameter	30
	Thickness	2
Seat Tube	Length	430
	Outer Diameter	32
	Thickness	2
Seat Stay	Length	450
	Outer Diameter	16
	Thickness	1.5
Chain Stay	Length	425
	Outer Diameter	16
	Thickness	1.5

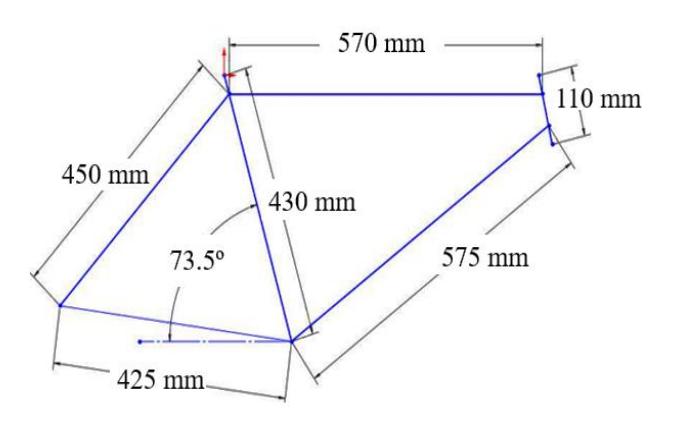


Fig.1 2D sketch of the bicycle frame.

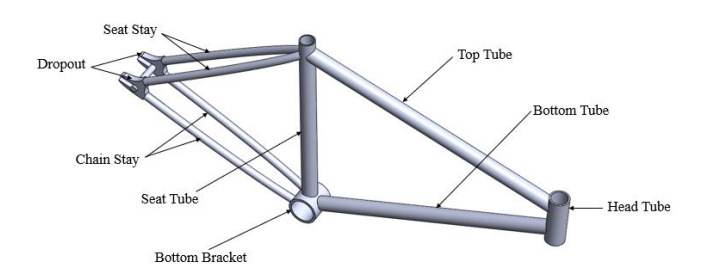


Fig.2 3D model of the bicycle frame.

2.3 Material Properties

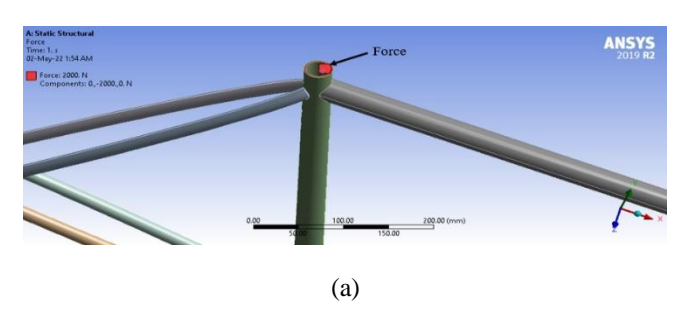
Aluminum 6061-T6, Steel and Titanium alloy are used as bicycle frame materials in this analysis. Table 2 shows the properties of these three materials. [16]

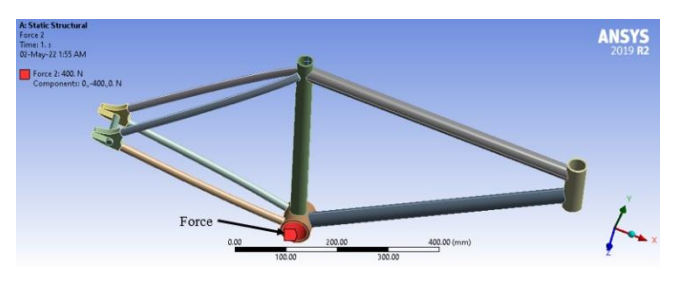
 Table 2 Material Properties.

26	Materials		
Material Properties	Steel	Aluminum 6061-T6	Titanium Alloy
Young's Modulus (MPa)	200000	71000	96000
Poison's Ratio	0.3	0.33	0.36
Density (kg/m³)	7850	2770	4620
Bulk Modulus (MPa)	166670	69608	114290
Shear Modulus (MPa)	76923	26692	35294

2.4 Boundary Condition

For Static start up load condition, 2000 N force is applied vertically on top of the seat tube and another 400 N force is applied vertically on the bottom bracket. Fixed support is applied on the dropout's connector and the inner surface of the head tube. Fig. 3(a), (b) and (c) represent the applied forces and fixed support for the Static start up load condition.





(b)

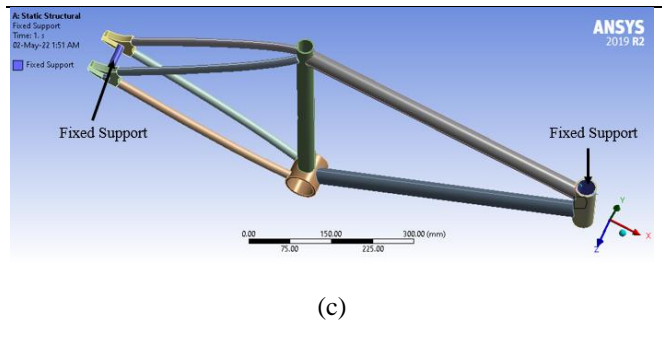
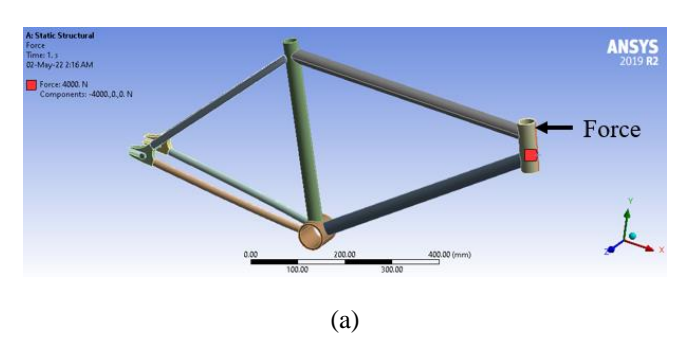


Fig.3 Boundary condition for static start up condition (a) force on top tube (b) force on bottom bracket (c) fixed support on head tube and dropout's connector.

For horizontal load condition, 4000 N force is applied horizontally at the head tube. Fixed support is applied on the dropout's connector and inner surface of the head tube. Fig. 4(a) and (b) exhibit the applied forces and fixed support location for the horizontal load condition.



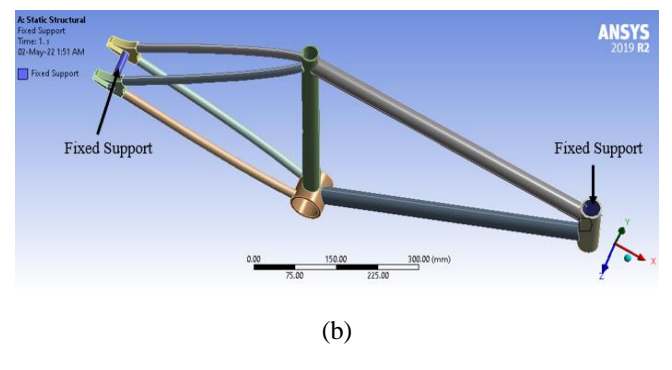
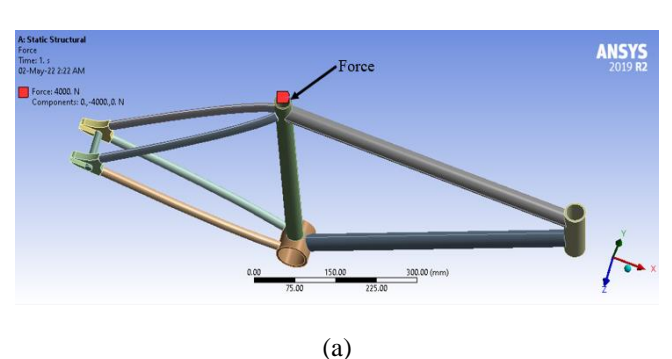


Fig.4 Boundary condition for horizontal load condition (a) force (b) fixed support.

For vertical load condition, 4000 N force is applied vertically on the seat tube. Fixed support is applied on the dropout's connector and inner surface of the head tube. Fig. 5(a) and (b) represent the applied forces and fixed support locations for the vertical load condition.



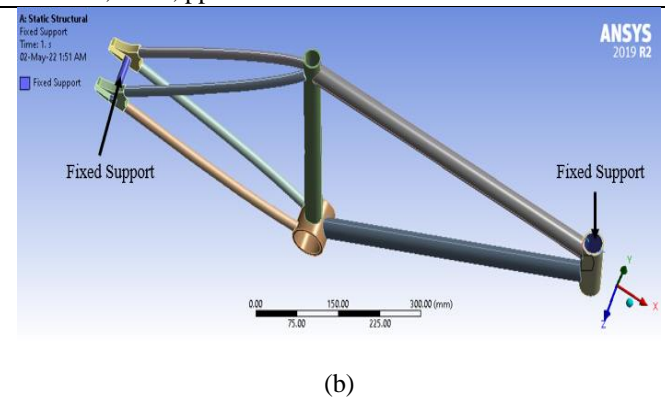


Fig.5 Boundary condition for vertical load condition (a) force (b) fixed supports.

2.5 Mesh Dependency Test

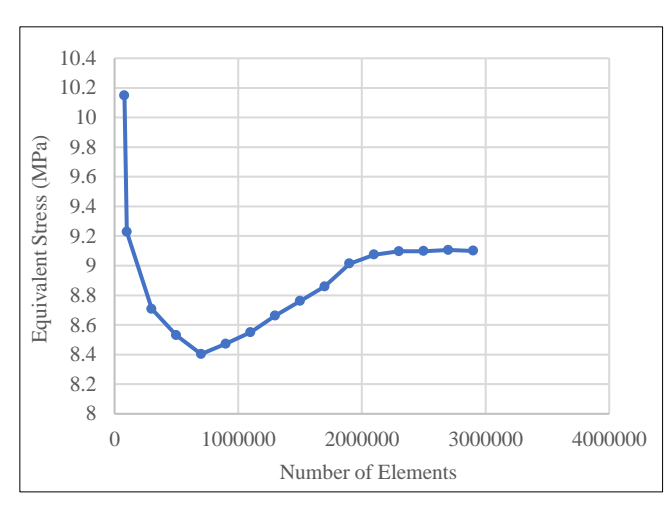


Fig.6 Mesh dependency check.

As shown in Fig. 6, the stress varies noticeably beneath the element count 2 million and stabilizes between the element count 2.2 million to 2.8 million. Considering the simulation accuracy and minimal duration of analysis, 2.6 million are chosen as the most optimal number of elements for the analysis.

2.6 Result Verification

To check the fidelity of the system of current work, a previously published research paper is chosen and verified. Table 3 shows the deviation of the present work from the published work. The deviation is less than 1% for all three load conditions. Fig. 7 presents the graphical comparison of present work and published paper. [10]

Table 3 Comparison of present work with published work

	Equivalent Stress		
Load Conditions	Published work (MPa)	Present work (MPa)	Deviation (%)
Static start up	1.32	1.322	0.15
Horizontal Load	19.86	19.816	0.22
Vertical Load	2.76	2.78	0.72

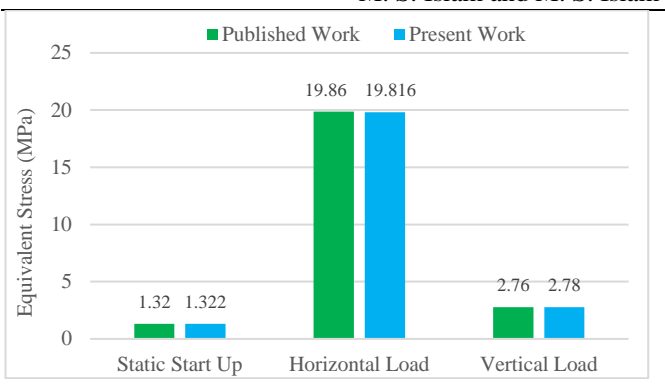


Fig.7 Comparison of present work with published work.

3. Result and Discussion

3.1 Static Start Up Condition

Fig. 8 represents the total deformation of the bicycle frame tubes for steel, aluminum and titanium. Among these three, tubes made of aluminum exhibit the highest deformation compared to steel and titanium, since the Young's Modulus of aluminum is 71 GPa, which is comparatively lower than the other two materials. The seat stay and seat tube of the frame experience the maximum deformation, as the load is applied almost axially to these components under static start up condition. Deformation of seat stay is 0.081 mm, 0.23 mm and 0.17 mm for steel, aluminum and titanium respectively. On the other hand, the top tube of the frame experiences the minimum deformation for all three materials. For steel, aluminum and titanium, these minimum deformation values are 0.025 mm, 0.071 mm and 0.053 mm respectively. Overall, aluminum made tubes experience approximately 180% greater deformation than the tubes made of steel, and experience 35% greater deformation than the tubes made of titanium.

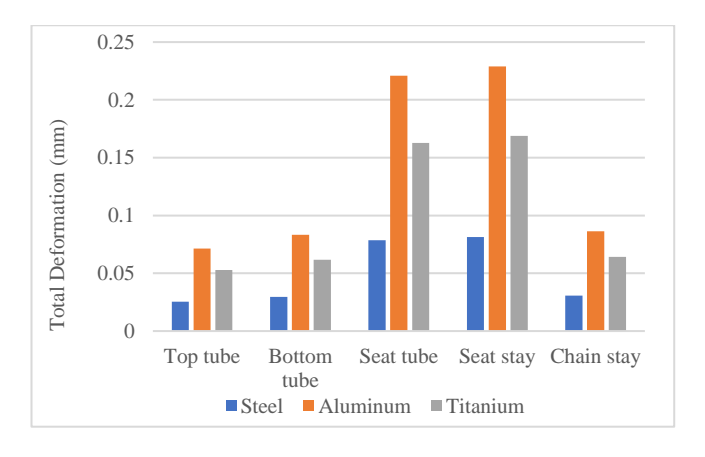


Fig.8 Variation of deformation under static start up condition.

3.2 Horizontal Load Condition

From Fig. 9 it can be seen that, the top tube of the bicycle frame exhibits the highest deformation under horizontal load condition. On the contrary, the chain stay experiences the lowest deformation across all three materials. All tubes made of aluminum experience the maximum deformation which is roughly 185% higher than steel made tubes. For steel, maximum and minimum deformation is 6.03×10^{-6} and 2.19×10^{-6} respectively.

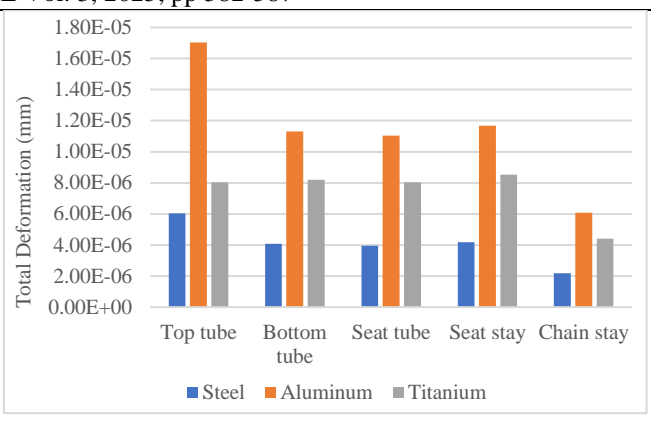


Fig.9 Variation of deformation under horizontal load condition.

3.3 Vertical Load Condition

From Fig. 10, the deformation pattern under vertical load condition closely like the deformation pattern in the static start up condition. The maximum and minimum deformation occurs in the seat stay and top tube. Steel made tubes exhibit the minimum deformation because of high stiffness. For aluminum, deformation ranges from 0.15 to 0.408; for steel it ranges from 0.0409 to 0.145, and for titanium deformation ranges from 0.0846 to 0.102.

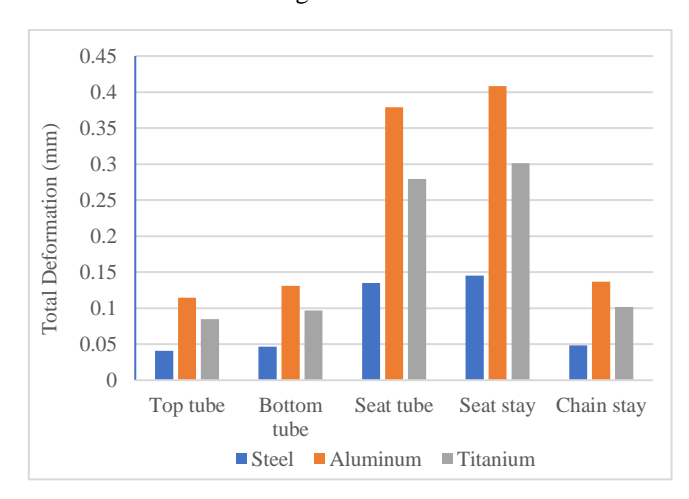


Fig.10 Variation of deformation under vertical load condition.

3.4 Graphical Analysis of Stress on Frame Tubes Under Different Load Conditions

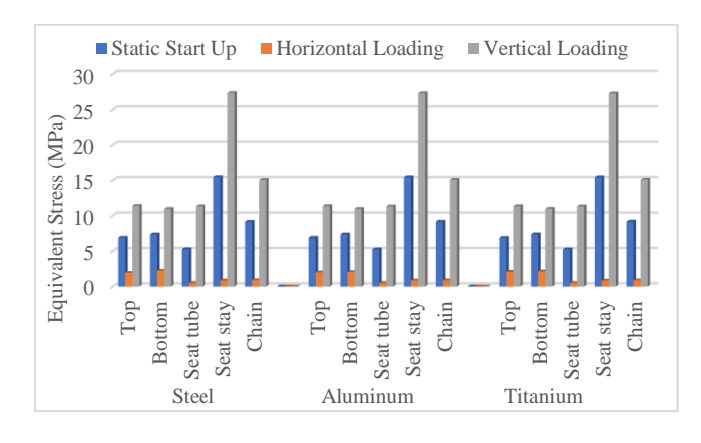
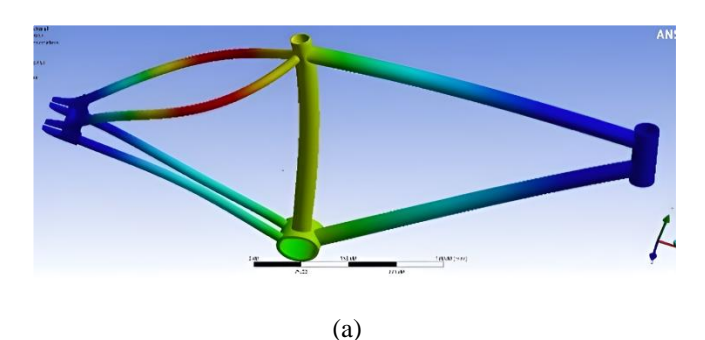
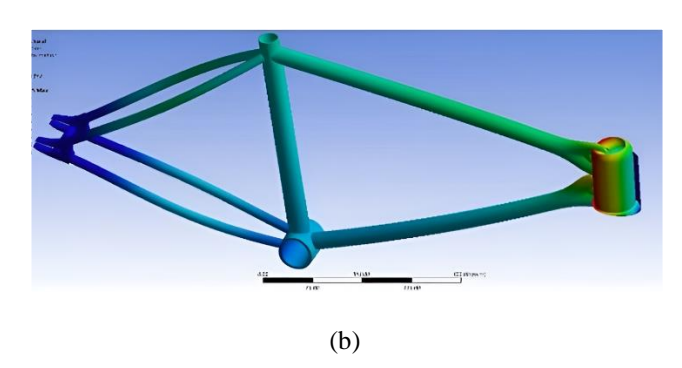


Fig.11 Stress variations on frame tubes.

Stress experienced by the five different tubes under different load conditions is shown in Fig. 11. For all three materials, the seat stay experiences the highest stress. The minimum stress occurs at the seat tube for all three materials and load conditions. Under horizontal load, the bottom tube endures the maximum stress across all materials.

3.5 Full frame analysis





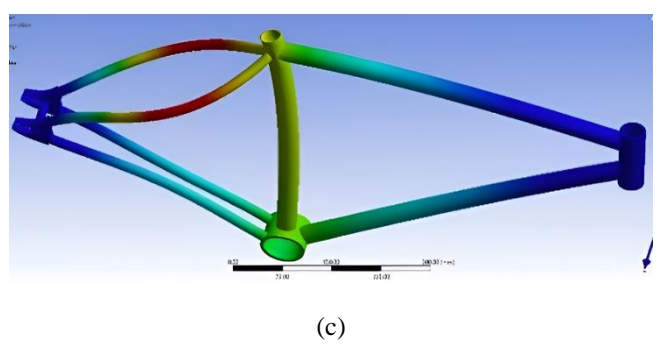


Fig.12 Deformation contours under (a) static start up (b) horizontal load (c) vertical load.

Fig. 8(a), (b) and (c) represent the deformation contours of full bicycle frame for three load conditions.

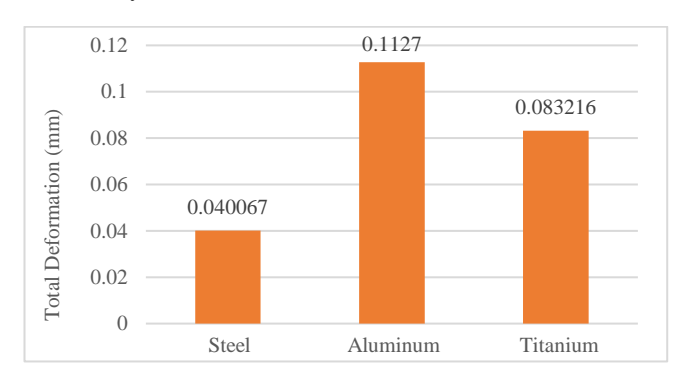


Fig.13 Deformation variation under static start up condition.

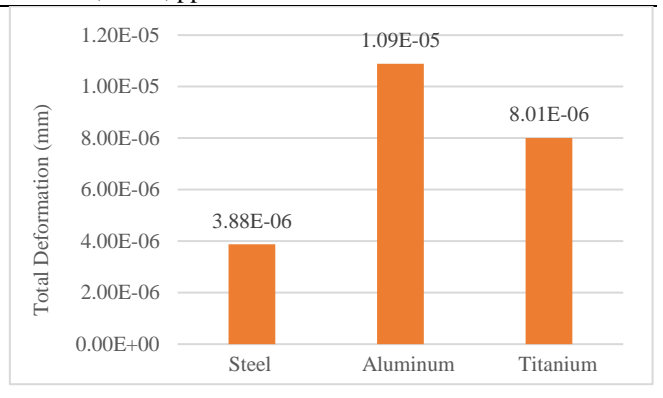


Fig.14 Variation of deformation under horizontal load condition.

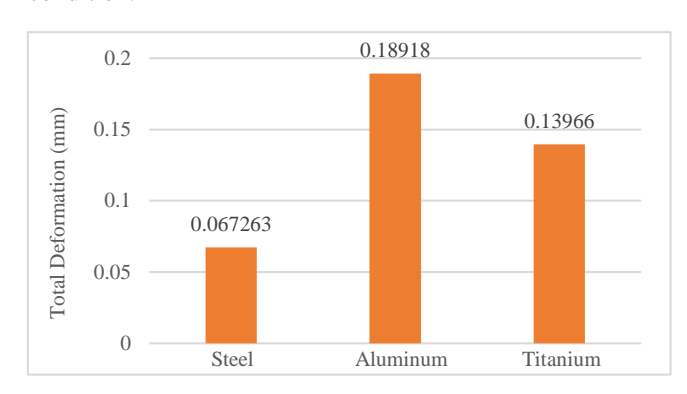


Fig.15 Variation of deformation under vertical load condition.

Fig. 13, 14 and 15 respectively shows the deformation experienced by the full bicycle frame under static start up, horizontal load and vertical load conditions. Due to the high stiffness of steel, it experiences the minimum deformation and aluminum made frame experiences the maximum. The deformation occurs in aluminum frame is approximately 180% greater than the deformation occurs in steel frame.

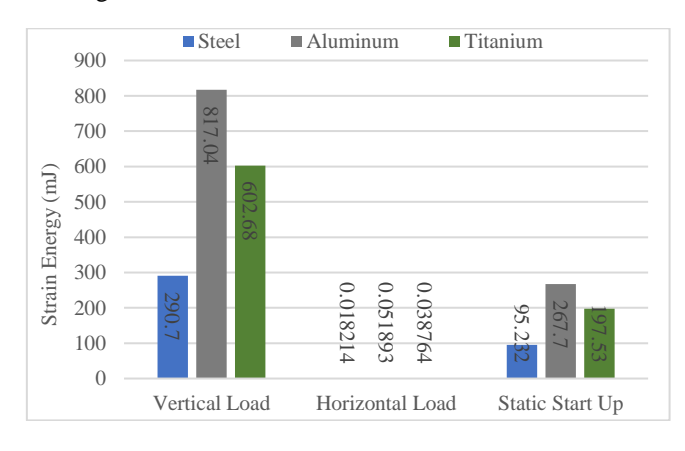


Fig.16 Strain energy variation of full frame.

The strain energy of the frame is analyzed using following formula:

$$U = \frac{1}{2}\sigma\varepsilon V \tag{5}$$

Due to the least deformation of steel frame, the strain energy is also minimum for steel and maximum for aluminum for all three load conditions, which is shown in Fig. 16.

4. Conclusion

In this research, static structural analysis was performed on bicycle frame tubes for three different materials, under three different load conditions. Steel frame tubes exhibited significantly higher resistance to deformation compared to the frame made of aluminum and titanium. Steel tubes exhibit approximately 65% less deformation than aluminum tubes and 51% less deformation than the titanium tubes. Although the aluminum frame is the lightest among the three, it showed the highest deformation for all frame tubes. In full bicycle frame analysis, the deformation in the aluminum made frame was approximately 180% greater than the steel made frame and 35% greater than the titanium made frame. Among all tubes, the seat stay, seat tube, and top tube displayed higher strain than other tubes, suggesting critical stress areas. Also the analysis express that the strain energy was highest in the aluminum frame and lowest in the steel frame, demonstrating significant material dependent variations in energy absorption.

References

- [1] Gupta, M. R., Rao, G. V. R. S., Analysis of Mountain Bike Frame By F.E.M, *IOSR Journal of Mechanical and Civil Engineering*, (*IOSR-JMCE*) *e-ISSN*, vol. 13, pp. 60–71, 2016.
- [2] Sajimsha, B., Kumar, A., Biju, S., Vishnu, P., Analysis of Mountain Bike Frames by ANSYS, *International Journal for Research in Applied Science & Engineering Technology*, vol. 7, pp. 1167–1175, 2019.
- [3] Covill, D., Allard, P., Drouet, J. M., Emerson, N., An Assessment of Bicycle Frame Behaviour under Various Load Conditions Using Numerical Simulations, in *Procedia Engineering*, Elsevier Ltd, pp. 665–670, 2016.
- [4] Kurhade, S., Kulkarni, S., Uplap, Y., Bhat, P., Ugale, A., Design and Analysis of Hybrid E-bike chassis, *International Research Journal of Engineering and Technology*, 2021.
- [5] Akhyar, Husaini, Iskandar, H., Ahmad, F., Structural simulations of bicycle frame behaviour under various load conditions, *Materials Science Forum*, Trans Tech Publications Ltd, pp. 137–147, 2019.
- [6] Mahanthesh, Kubasad, P. R., Kirankumar, Numerical Analysis for a Bicycle Frame made of Mild Steel and Composite, *International Journal for Research Trends and Innovation (IJRTI)*, vol. 3, ISSN: 2456-3315, 2018.
- [7] Varghese, A. S., Sreejith, Structural Analysis of Bicycle Frame Using Composite Laminate,

- International Journal of Engineering Trends and Technology, vol. 28, ISSN: 2231-5381, 2015.
- [8] Pawar, R. J., Kolhe, K. P., Vibrational Analysis of Bicycle Chassis, *IJIRST-International Journal* for Innovative Research in Science & Technology, vol. 3, ISSN: 2349-6010, 2016.
- [9] Devaiah, B. B., Purohit, R., Rana, R. S., Parashar, V., Stress Analysis of a Bicycle Frame, In: proceedings of 8th International Conference Material Properties and Characterization, 16-18 March, Hyderabad, India, 2018.
- [10] Mishra, K. K., Chaturvedi, V., Stress analysis of bicycle frame using ansys, *International Research Journal of Engineering and Technology*, vol. 08, Issue: 05, 2021.
- [11] Khutal, K., Simhachalam, B., Jebaseelan, D. D., Design Validation Methodology for Bicycle Frames Using Finite Element Analysis, In: proceedings of 6th International Conference on Mechanical, Materials and Manufacturing, 12-14 October, Boston, USA, 2020.
- [12] Covill, D., Blayden, A., Coren, D., S. Begg, S., Parametric finite element analysis of steel bicycle frames: The influence of tube selection on frame stiffness, In: Procedia Engineering 7th Asia-Pacific Congress on Sports Technology, 23-25 September, Barcelona, Spain, 2015.
- [13] Sarath, Deepak, A., Daniel, N. S., Jinuchandran, Hrishikesh, Stress Analysis of Bicycle Frame using Different Materials by FEA, *GRD Journal for Engineering*, vol. 6, Issue 7, 2021.
- [14] Logan, D. L., A First Course in the Finite Element Method, CENGAGE Learning, 4th Ed., 748-751, 2009.
- [15] https://bikeinsights.com/bikes/5dcdf6bad2bfe90017
 44b7b5-waterford-precision-cycles-adventure-cycle?build=canti&version=2019
 (22 January, 2022).
- [16] Ashby, M., Material property data for engineering materials, Ansys EDUCATION RESOURCES, Ed. 5, England, 2021.

NOMENCLATURE

 ε : Strain

 σ : Stress, MPa

E: Modulus of Elasticity, MPa

v : Poisson's ratio

V: Volume of the material, mm³